High Voltage

Research Article

IET Journals
The Institution of Engineering and Technology

Received signal strength indication-based localisation method with unknown path-loss exponent for HVDC electric field measurement

ISSN 2397-7264
Received on 30th May 2017
Revised 15th June 2017
Accepted on 24th June 2017
E-First on 27th July 2017
doi: 10.1049/hve.2017.0085
www.ietdl.org

Xiaolan Gu[1,2], Yong Cui[1] ✉, Qiusheng Wang[1], Haiwen Yuan[1], Luxing Zhao[3], Guifang Wu[3]

[1]*School of Automation Science and Electrical Engineering, Beihang University, Beijing 100191, People's Republic of China*
[2]*Graduate School of System and Information Engineering, University of Tsukuba, Ibaraki 305-8577, Japan*
[3]*High Voltage Department, China Electrical Power Research Institute, Beijing 100192, People's Republic of China*
✉ *E-mail: cuiyong@buaa.edu.cn*

Abstract: The electric field environment under high-voltage direct current (HVDC) transmission lines is an important design consideration. In the wireless sensor networks for electric field measurement system under the HVDC transmission lines, it is necessary to obtain the electric field distribution with multiple sensors. The accurate localisation of sensing nodes is essential to the analysis of measurement results. However, most current techniques are limited to constant measurement environment with fixed and known path-loss exponent. Here, the authors report a localisation method based on received signal strength indication with unknown path-loss exponent for the localisation of one-dimensional linear topology wireless networks in the electric field measurement system. The optimisation method is utilised to obtain the optimal pass-loss parameter without involving the previous environment parameters. Afterwards, simulations are employed to demonstrate the feasibility and the effectiveness of the proposed method by comparing with other methods.

1 Introduction

Compared with the high-voltage alternating current (HVAC) transmission system, high-voltage direct current (HVDC) transmission system is a better choice for long-distance bulk power transmission, and is able to send vast amounts of electricity over very long distances with less power losses and lower environmental impact [1–4]. Several ±800 and ±1000 kV HVDC transmission systems are now in commercial operation in some countries [5]. According to the planning of some grid cooperation, about 30 HVDC transmission projects will be constructed by 2020 in the world.

With the large-scale implementations of HVDC transmission lines, the environmental impacts due to electromagnetic waves have become a focus of public attention in the following technical parameters: electric field [6–8], ion current density, space charge density [9], radio interference [10, 11], audible noise [12, 13], corona discharge [14–17] etc. In contrast to the HVAC transmission lines, the electric field under HVDC lines is greatly enhanced when a corona discharge occurs and an accurate and efficient measurement method is needed to assure the system follows the electromagnetic environmental standard. To evaluate the power system and control the electric field to satisfy the electromagnetic environmental standard, an accurate and efficient measurement method needs to be employed.

To measure the electric field distribution at different positions under transmission lines, electric field sensors are arrayed along the direction perpendicular to the transmission lines. The wireless node is connected with electric field sensor through twisted-pair braid shielded cable. The wireless nodes' primary function is to acquire and process the analogy signal of the sensor and send the electric field result to the remote computer. The key requirement of the measurement system is to correlate the received electric field data with the locations of the electric field sensors. Therefore, it is crucial to precisely and automatically obtain position of sensors in the wireless sensor networks. However, the most challenge is that the field test environment under the HVDC transmission lines is extremely complex and variable. Normally, the field test environment can be constituted by different types of circumstances, such as grass, undulating land, open flat. Moreover, the electromagnetic interference, terrain, vegetation and other unknowable factors are likely to cause random interference on the localisation result [18]. Therefore, the localisation algorithm for electric field measurement system should have strong self-adaptivity to various test environments.

Most current wireless sensor networks (WSN) localisation algorithms, which rely on distances estimation, are based on the time of arrival [19], time difference of arrival [20], angle of arrival [21], and received signal strength indication (RSSI) [22]. Owing to low cost, low-energy consumption, and the free of additional devices, the RSSI-based localisation technique has been widely used in practical applications. The classical RSSI-based methods are triangle centroid method [23] and received signal strength difference (RSSD) method [24]. In these RSSI-based methods, the radio propagation model parameters are fixed and known. However, in the application of electric field measurement, radio propagation model parameters are variable and unknown. Thus, we report an RSSI-based localisation algorithm, which is self-adaptive to unknown model parameters. Furthermore, we introduce the Cramer–Rao lower bound (CRLB) to show self-adaptability of the algorithm to different test environment.

2 Localisation method with unknown path-loss exponent

In electric field measurement under HVDC transmission lines [25], the electric field sensors [26] are arranged on the straight line being perpendicular to the transmission lines (refer to Fig. 1), to obtain the electric field strength distribution. Considering the localisation problem in wireless sensor networks, most of the algorithms are based on two-dimensional plane coordinated by (x, y), and the simplified diagram is shown in Fig. 2. Since all the nodes are located in a straight line, the localisation problem can be simplified as a one dimensional. Hence, only one coordinate is used to indicate the location of each node.

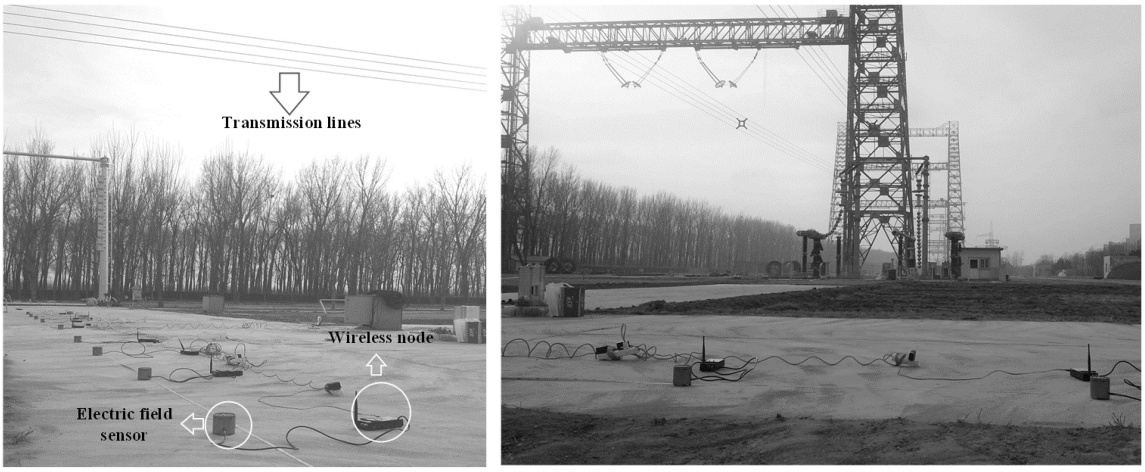

Fig. 1 *Electric field measurement under HVDC transmission lines*

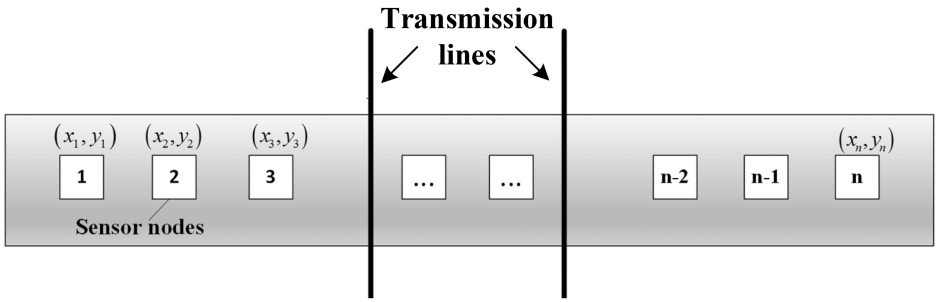

Fig. 2 *Simplified diagram of sensor nodes distribution in HVDC application*

Table 1 The value of η and σ with different environments

Propagation environment	Path-loss η	Shadowing deviation σ
500 kv substation (LOS)	2.42	3.12
500 kv substation (NLOS)	3.51	2.95
underground transformer vault (LOS)	1.45	2.45
underground transformer vault (NLOS)	3.15	3.19
main power room (LOS)	1.64	3.29
main power room (NLOS)	2.38	2.25

LOS means line-of-sight and NLOS means non-LOS.

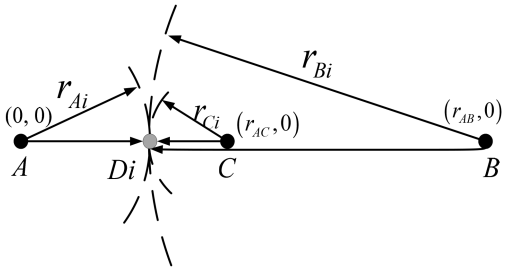

Fig. 3 *Simplified diagram of the localisation model*

2.1 Wireless signal logarithmic decrement model

The non-linear equations for distance measurement-based location estimation can be related to RSSI values via the classical narrowband radio propagation path-loss model [27]

$$P(d) = P(d_0) - 10\eta\log_{10}\left(\frac{d}{d_0}\right) + v \tag{1}$$

where $P(d)$ is the measured RSSI at the receiver, $P(d_0)$ is the RSSI value received at a reference distance d_0 from the source node (in general $d_0 = 1$ m), v denotes the measurement noise which assumed to be white Gaussian noise with zero-mean, i.e. $v \sim N(0, \sigma^2)$. In addition, η is the path-loss exponent of the environment. The value of η is vary from 2 to 6 in different regions and the value is shown in Table 1 [28].

For convenience, we assume $d_0 = 1$ m and denote $\alpha = 10\eta, P_0 = P(d_0)$. Thus, (1) can be rewritten as

$$P(d) = P_0 - \alpha\log_{10}(d) \tag{2}$$

Then the estimated distance is calculated by

$$d = 10^{(P_0 - P(d))/\alpha} \tag{3}$$

In practical applications, the measured RSSI is highly environmentally sensitive, and the multipath effects of signal transmission and obstacles blocking will make the measured RSSI fluctuate. The influence of the noises and the imprecise prior parameters (α and P_0) may increase the estimation error for nodes localisation. To get rid of the influence of inaccurate value of P_0, the RSSD can be used to estimate the unknown distance [28]. However, the path-loss exponent η is still a priori value in this method. Therefore, it is unable to reflect the environmental impact on wireless signals when practical environment changes, which will cause even larger localisation errors.

Considering all the factors above, we propose an RSSI-based localisation algorithm with unknown pass-loss exponent (UPLE) to self-adaptively estimate the model parameters.

2.2 The UPLE estimation method

In the localisation model, three anchor nodes A, B, C are used to estimate the unknown nodes (D_i). The simplified diagram is shown in Fig. 3. The coordinates of anchor nodes A, B, C are $(0, 0), (r_{AB}, 0), (r_{AC}, 0)$, respectively. We assume the unknown node D_i is located at $(d, 0)$. The RSSI values of D_i from anchors A, B, C are denoted by P_{Ai}, P_{Bi}, P_{Ci}, respectively.

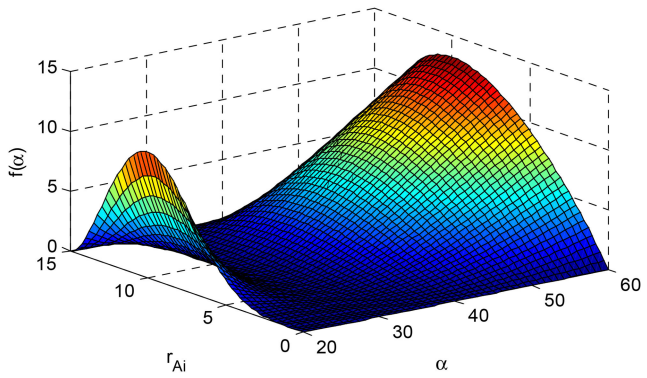

Fig. 4 *The value of $f(\alpha)$ with different D_i*

Table 2 The pseudo-code of the proposed UPLE algorithm

UPLE algorithm: to estimate the localisation when pass-loss exponent is unknown

Input: anchors positions $r_{AB}, r_{AC}$and received signal strengths P_{Ai}, P_{Bi}, P_{Ci}

1: **if** $P_{Ai} > P_{Bi}$, **then**

2: Obtain the optimal α by solving the optimisation problem (8)

3: Calculate x_1 and x_2 via (6) with the solved α

4: **else**

5: Calculate $r_{BC} = r_{AB} - r_{AC}$

6: Obtain the optimal α by solving the optimisation problem (9)

7: Calculate x_1 and x_2 via (7) with the solved α

8: **end if**

Output: the estimated position $d = (x_1 + x_2)/2$

According to the path-loss model in (1), we have the following formulas when localising the unknown node through anchors A, B and anchors A, C, respectively

$$P_{Ai} - P_{Bi} = \alpha \log_{10} \frac{r_{Bi}}{r_{Ai}}, \quad P_{Ai} - P_{Ci} = \alpha \log_{10} \frac{r_{Ci}}{r_{Ai}} \tag{4}$$

Without loss of generality, we assume that unknown node D_i is located between anchors A and C, i.e. $r_{Ai} < r_{AC}$. Therefore, the relationships $r_{Ai} = r_{AB} - r_{Bi}, r_{Ai} = r_{AC} - r_{Ci}$ are obvious due to the straight-line locations. For convenience, we denote $x_1 = r_{Ai} = r_{AB} - r_{Bi}$ and $x_2 = r_{Ai} = r_{AC} - r_{Ci}$. Then, (4) can be rewritten as

$$P_{Ai} - P_{Bi} = \alpha \log_{10} \frac{r_{AB} - x_1}{x_1}, \quad P_{Ai} - P_{Ci} = \alpha \log_{10} \frac{r_{AC} - x_2}{x_2} \tag{5}$$

or equivalently

$$x_1 = \frac{r_{AB}}{1 + 10^{(P_{Ai} - P_{Bi})/\alpha}}, \quad x_2 = \frac{r_{AC}}{1 + 10^{(P_{Ai} - P_{Ci})/\alpha}} \tag{6}$$

where x_1 and x_2 represent the estimated value of r_{Ai} via different two pairs of anchor nodes, respectively, and both of them are functions respected to α. In a similar way, if D_i is located between anchors B and C, i.e. $r_{Ai} > r_{AC}$, the formulas are represented as

$$x_1 = \frac{r_{AB}}{1 + 10^{(P_{Ai} - P_{Bi})/\alpha}}, \quad x_2 = r_{AB} - \frac{r_{BC}}{1 + 10^{(P_{Bi} - P_{Ci})/\alpha}} \tag{7}$$

If there is no noise of received signal strengths P_{Ai}, P_{Bi}, P_{Ci}, we can see that $x_1 = x_2$. However, when considering the fluctuant of signal strengths, the gap between x_1 and x_2 will be related with α. As a result, this gap can be minimised if we choose an appropriate value of α. Then, we resort to the optimisation model to obtain the optimal α.

2.3 The optimal α in UPLE algorithm

Without loss of generality, we assume the unknown node D_i is located between anchors A and C, i.e. $r_{Ai} < r_{AC}$. Then (6) will be used to estimate the optimal value of α. Since the range of α is 20–60, the following objective function is introduced:

$$\begin{aligned} \min \quad & f(\alpha) = \left(\frac{r_{AB}}{1 + 10^{(P_{Ai} - P_{Bi})/\alpha}} - \frac{r_{AC}}{1 + 10^{(P_{Ai} - P_{Ci})/\alpha}} \right)^2 \\ \text{s.t.} \quad & 20 \le \alpha \le 60 \end{aligned} \tag{8}$$

where r_{AB} and r_{AC} are the specified anchor positions, P_{Ai}, P_{Bi}, P_{Ci} are the measured RSSI values of D_i from anchors A, B, C, respectively. The graph of objective function $f(\alpha)$ with different r_{Ai} is shown in Fig. 4, where we assume that $r_{AB} = 30\,\text{m}, r_{AC} = 15\,\text{m}, \alpha = 30$, the position of D_i is between A and C (means $0 < r_{Ai} < r_{AC} = 15\,\text{m}$), and the influence of the noise is ignorable. In Fig. 4, we can see that $f(\alpha)$ is a one-peak function with respect to α, which means the unique minimum point of this objective function. In addition, $f(\alpha)$ reaches at the minimum when the value of α nears 30, which is the true value of the parameter. Since there is only one extreme point for a certain unknown node, we can use a common operational algorithm by Opt Toolbox to find the optimal value. In this paper, the single-variable bounded nonlinear function minimisation is applied for this optimisation problem, referred as *fminbnd* function in MATLAB, where the default parameter values are utilised.

In a similar way, if D_i is located between anchors B and C, i.e. $r_{Ai} > r_{AC}$, we can get the following objective function from (7):

$$\begin{aligned} \min \quad & f(\alpha) = \left(\frac{r_{AB}}{1 + 10^{(P_{Ai} - P_{Bi})/\alpha}} - r_{AB} + \frac{r_{BC}}{1 + 10^{(P_{Bi} - P_{Ci})/\alpha}} \right)^2 \\ \text{s.t.} \quad & 20 \le \alpha \le 60 \end{aligned} \tag{9}$$

which has the similar properties as (8). On the other hand, we can use the values of P_{Ai} and P_{Bi} to judge D_i is located between whether anchors A and C, or anchors B and C. Since longer distance yields weaker received signal strength, the unknown node D_i is located closer to anchor A than B when $P_{Ai} > P_{Bi}$, and vice versa.

In summary, the parameter α can be obtained via (8) or (9), then x_1 and x_2 are calculated by (6) or (7). To balance the potential estimation errors of x_1 and x_2, we use the mean value of them as the location of the unknown node D_i, i.e. $d = (x_1 + x_2)/2$. Finally, the proposed UPLE algorithm for localisation when pass-loss model parameter is unknown is summarised in Table 2.

Compared with the triangle centroid method or RSSD method, the proposed UPLE is able to localise the unknown nodes without the prior value of parameter α. Hence, the proposed method is more self-adaptive when localising unknown nodes using measured RSSI values in practical applications.

2.4 CRLB analysis with measurement noise

Considering the measurement noise of RSSI values, the CRLB is introduced for comparisons with the simulation results. The CRLB provides a lower limit on the covariance matrix of an unbiased estimator which can be defined as [27]

$$\text{cov}\left(\hat{\theta}\right) - \tilde{F}_\theta^{-1} \ge 0 \tag{10}$$

where cov() is the covariance matrix of the unknown vector $\hat{\theta}$, the symbol ≥ 0 means positive semi-definiteness of a matrix and $\tilde{F}_\theta$ is the Fisher information matrix, which is defined as

$$\tilde{F}_\theta = -E[\nabla_\theta(\nabla_\theta \ln f(x_i, \theta))] \tag{11}$$

where $E[]$ is the mathematical expectation and ∇_θ denotes the partial differential respect to variable θ. From the narrowband radio

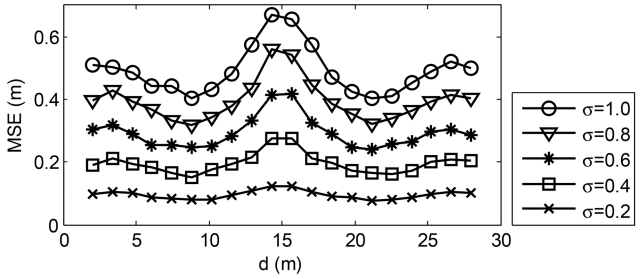

Fig. 5 *MSE values of different unknown nodes under different σ when $\alpha = 30$*

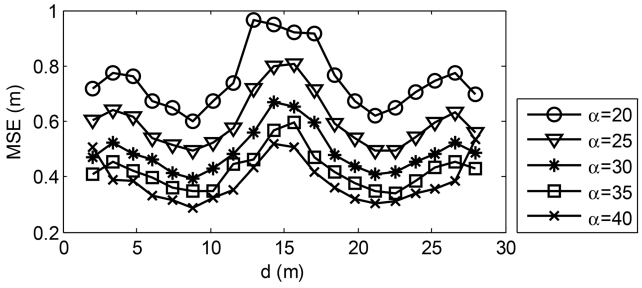

Fig. 6 *MSE values of different unknown nodes under different α when $\sigma = 1$*

Table 3 The mean value of estimated α via UPLE method at certain positions when $\sigma = 1$

True α		20	25	30	35	40
estimated α	at $d = 3$ m	19.75	24.89	29.96	34.98	39.98
	at $d = 5$ m	20.10	24.98	30.08	34.88	39.94
	at $d = 8$ m	19.91	24.93	29.92	35.09	40.02
	at $d = 10$ m	19.90	24.99	29.90	34.87	40.03
	at $d = 13$ m	19.80	24.76	29.57	34.53	39.55

propagation path-loss model in (1), the CRLB for unbiased distance estimators can be expressed as [29]

$$\sqrt{\mathrm{var}\left(\hat{d}\right)} \geq \frac{(\ln 10)\cdot\sigma\cdot d}{10\eta} \tag{12}$$

where $\hat{d}$ represents an unbiased estimate for the distance d. Afterwards, the CRLB line will be used in simulation parts.

3 Results

To test the performance of UPLE method, we compare it with the following two classical RSSI-based localisation methods:

i. Triangle centroid method [24]: It estimates the positions of unknown nodes by determining the centroid of an artificial triangle, which is constructed by connecting three intersections of distance circles of three anchor nodes. Since the localisation problem is simplified as a one-dimensional problem for HVDC electric field measurement, the formula of triangle centroid method is arranged as

$$d = \begin{cases} [r_{Ai} + (r_{AC} - r_{Ci}) + (r_{AB} - r_{Bi})]/3, & P_{Ai} > P_{Bi} \\ r_{AC}, & P_{Ai} = P_{Bi} \\ [r_{Ai} + (r_{AC} + r_{Ci}) + (r_{AB} - r_{Bi})]/3, & P_{Ai} < P_{Bi} \end{cases} \tag{13}$$

where r_{Ai}, r_{Bi}, r_{Ci} are the distances between unknown node D_i and anchor nodes A, B, C, respectively, and they are calculated via (3) with measured P_{Ai}, P_{Bi}, P_{Ci} and prior model parameter α.

ii. RSSD method [28]: It localises the unknown nodes via the RSSD between anchors. For the sensor nodes localisation problem for electric field measurement under HVDC lines, the estimated position is calculated by

$$d = \frac{r_{AB}}{1 + 10^{(P_{Ai} - P_{Bi})/\alpha}} \tag{14}$$

Note that the prior value of parameter α is necessary for triangle centroid method and RSSD method, while the proposed one is able to estimate the optimal α then localise the unknown nodes.

In this section, the mean-squared error (MSE) is introduced to quantify the error between the estimated position and the true position:

$$\mathrm{MSE}\left(\mathbf{d}, \hat{\mathbf{d}}, N\right) = \frac{\| \mathbf{d} - \hat{\mathbf{d}} \|_2}{\sqrt{N}} \tag{15}$$

where $\mathbf{d} \in \mathfrak{R}^N$ is a vector constituted by the true positions and $\hat{\mathbf{d}} \in \mathfrak{R}^N$ is the estimated vector, each element of $\hat{\mathbf{d}}$ is the outcome of each test. In addition, $\| \cdot \|_2$ is the two-norm of a vector and integer $N > 0$ is the test number.

3.1 Performances of the proposed UPLE method

We test the performances of the proposed method when anchors are located in $A(0,0), B(30,0), C(15,0)$, i.e. $r_{AB} = 30$ m, $r_{AC} = 15$ m. The test number is $N = 1000$. The MSE values of estimated positions with different σ when true model parameter $\alpha = 30$ are shown in Fig. 5. We see that the values of MSE is smaller than 0.7 m when σ is no more than 1. In addition, the positions which are far away from the anchors (at 0, 15 and 30 m) possess a better performance. This phenomenon occurs due to the bigger curvature (see Fig. 4) on these positions of the objective function in (8).

On the other hand, the MSE values of estimated locations under different α when $\sigma = 1$ are shown in Fig. 6, and the estimated values of α are listed in Table 3. We see that the estimated α is much close to the true values at different positions and on different circumstances. The results illuminate the effectiveness of the optimisation-based estimation method for α in UPLE.

3.2 Performance comparisons with classical methods

We compare the performances among the triangle centroid method (denoted as tri-centroid), RSSD method, and the proposed UPLE method. Note that a prior value of α is necessary in the two classical methods, while UPLE is able to estimate model parameter α. The MSE values for two cases ($r_{AB} = 30$ m, $r_{AC} = 15$ m and $r_{AB} = 100$ m, $r_{AC} = 50$ m) with $\sigma = 1$ and $\alpha = 30$ are shown in Figs. 7 and 8, respectively. We see a relatively stable and lower MSE values for different d of the UPLE method. The localisation accuracy of Tri-centroid method is lower than UPLE for all d. The RSSD possesses a higher accuracy when unknown nodes close to anchor node A or B, but a much lower accuracy when unknown nodes are located far from A and B.

The results of MSE mean-values under different standard deviation σ are listed in Table 4. We can see that the values of MSE of the three methods will be increased when σ is enlarged or the localisation range is extended. However, the UPLE method has a lowest mean-value for different cases (different σ or range). That illuminates the superiority of the proposed method.

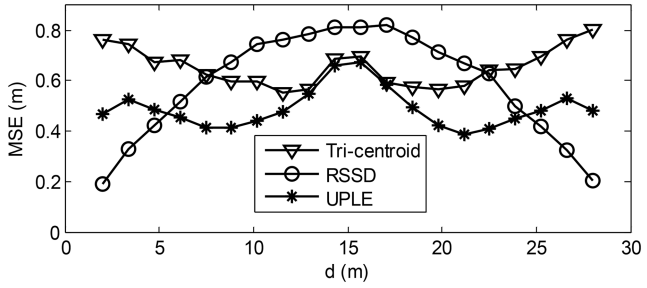

Fig. 7 *MSE comparisons when* $r_{AB} = 30\,\text{m}, r_{AC} = 15\,\text{m}$ *with* $\sigma = 1$ *and* $\alpha = 30$

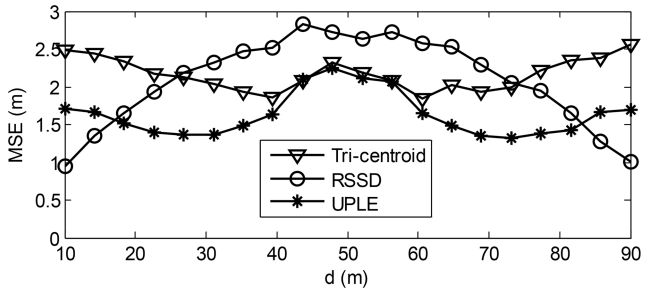

Fig. 8 *MSE comparisons when* $r_{AB} = 100\,\text{m}, r_{AC} = 50\,\text{m}$ *with* $\sigma = 1$ *and* $\alpha = 30$

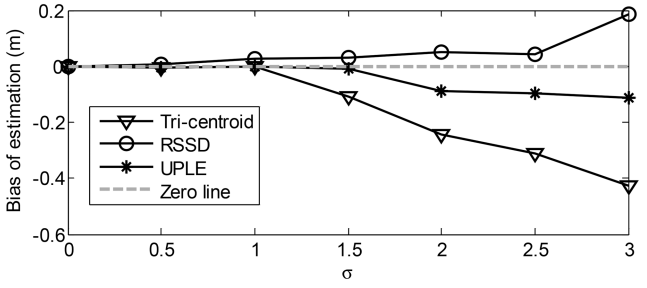

Fig. 9 *The estimation bias of three algorithms at* $d = 7\,\text{m}$ *with different* σ

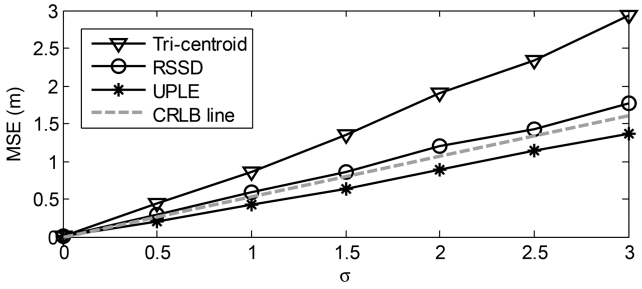

Fig. 10 *The estimation bias of three algorithms at* $d = 7\,\text{m}$ *with different* σ

experiment, we test the algorithm performance under various

Table 4 Mean value of MSE for two cases ($r_{AB} = 30\,\text{m}, r_{AC} = 15\,\text{m}$ and $r_{AB} = 100\,\text{m}, r_{AC} = 50\,\text{m}$)

		Mean-value of MSE, m			
		$\sigma = 0.5$	$\sigma = 1.0$	$\sigma = 1.5$	$\sigma = 2$
$r_{AB} = 30\,\text{m}, r_{AC} = 15\,\text{m}$	tri-centroid	0.325	0.663	1.003	1.359
	RSSD	0.292	0.594	0.878	1.172
	UPLE	0.241	0.494	0.746	1.017
$r_{AB} = 100\,\text{m}, r_{AC} = 50\,\text{m}$	tri-centroid	1.056	2.164	3.294	4.494
	RSSD	1.027	2.077	3.104	4.134
	UPLE	0.805	1.660	2.494	3.424

Table 5 The mean value of MSE with changeable model parameter

	Mean value of MSE (m) when $\alpha_0 = 30$			Mean value of MSE (m) when $\alpha_0 = 50$		
	$\sigma_\alpha = 1$	$\sigma_\alpha = 2$	$\sigma_\alpha = 5$	$\sigma_\alpha = 1$	$\sigma_\alpha = 2$	$\sigma_\alpha = 5$
tri-centroid	1.09	1.93	5.46	0.80	1.39	3.70
RSSD	0.89	1.46	3.33	0.67	1.08	2.54
UPLE	0.73	1.21	2.88	0.55	0.89	2.26

3.3 Performances with CRLB line at a certain position

We test the performances at a certain position $d = 7\,\text{m}$ for the case that $r_{AB} = 30\,\text{m}, r_{AC} = 15\,\text{m}$. First, we define biasness as $\text{Bias} = \sum_{i=1}^{N}\left(\hat{d}_i - d_i\right)/N$, where $\hat{d}_i$ and d_i are the ith estimated position and true position, respectively, and N is the test number. The results when $N = 1000$ are shown in Fig. 9, from which we know that all of the three methods are biased estimators.

Then, the MSE values of three algorithms are shown in Fig. 10. When the value of σ is increasing, the UPLE possesses a lower MSE value than other methods, which reflects the effectiveness of it. Besides, a line of CRLB, which is added in Fig. 10, which is computed via (12). Node that CRLB is the lower bound of all the unbiased estimations which are based on (2). The MSE values of UPLE can even go below CRLB, which results from the biasness of this estimator. This performance indicates that the biased UPLE estimator possesses a better performance than any unbiased estimators.

3.4 Performances with fluctuant model parameter

In practical applications, the value of parameter α often fluctuates due to the random interferences in complex circumstance. In this model parameter $\alpha = \alpha_0 + \Delta\alpha$, where α_0 is the original parameter, $\Delta\alpha$ is a fluctuate variable assumed to obey the normal distribution with zero-mean and standard deviation σ_α, i.e. $\Delta\alpha \sim N(0, \sigma_\alpha)$. The mean value of MSE via different algorithms is listed in Table 5. Since the UPLE method is able to estimate the model parameter α, the fluctuate of α only influences the measured RSSI values. However, the inaccurate α also affects the pass-loss model in the tri-centroid and RSSD method. The results validate the practicability of the proposed method.

4 Conclusion

This paper has proposed an RSSI-based localisation algorithm (named UPLE) in which the radio propagation path-loss model parameter is not pre-required. Several kinds of factors are considered, including that the signal strength is susceptible to be influenced, and the value of pass-loss model parameter is variable. The UPLE method seeks the optimal parameter to minimise the gap between estimation results of different pairs of anchor nodes. This method can effectively restrain the influence coming from practical circumstance. Based on simulation analysis, the estimation error of the proposed UPLE localisation method is smaller than its counterparts under complex measurement

environment, including different levels of interference, different distribution range of sensor nodes, various pass-loss model parameter. Besides, the biased UPLE method with the lower bound of unbiased estimations is better than CRLB line.

5 Acknowledgments

This work was supported in part by China Aviation Science Foundation (2015ZD51051), National Natural Science Foundation of China (61273165), and SGCC Science and Technology Project of China (GY71-16-010).

6 References

[1] Maruvada, P.S.: 'Influence of wind on the electric field and ion current environment of HVDC transmission lines', *IEEE Trans. Power Deliv.*, 2014, **29**, (6), pp. 2561–2569

[2] An, T., Tang, G., Wang, W.: 'Research and application on multi-terminal and DC grids based on VSC-HVDC technology in China', *High Voltage*, 2017, **2**, (1), pp. 1–10

[3] Zhen, Y., Cui, X., Lu, T., *et al.*: 'Ion flow field analysis considering the finite conductivity of the building near HVDC transmission lines', *IEEE Trans. Magn.*, 2015, **51**, (3), pp. 1–4

[4] Wang, Q., Kundur, D., Yuan, H., *et al.*: 'Noise suppression of corona current measurement from HVdc transmission lines', *IEEE Trans. Instrum. Meas.*, 2016, **65**, (2), pp. 264–275

[5] Sun, H., Cui, X., Du, L.: 'Electromagnetic interference prediction of ±800 kV UHVDC converter station', *IEEE Trans. Magn.*, 2016, **52**, (3), pp. 1–4

[6] Zhen, Y., Cui, X., Lu, T., *et al.*: 'A laboratory study on the ion-flow field model of the DC wires in stable wind', *IEEE Trans. Power Deliv.*, 2015, **30**, (5), pp. 2346–2352

[7] Lu, T., Feng, H., Zhao, Z., *et al.*: 'Analysis of the electric field and ion current density under ultra high-voltage direct-current transmission lines based on finite element method', *IEEE Trans. Magn.*, 2007, **43**, (4), pp. 1221–1224

[8] Lu, T., Feng, H., Cui, X., *et al.*: 'Analysis of the ionized field under HVDC transmission lines in the presence of wind based on upstream finite element method', *IEEE Trans. Magn.*, 2010, **46**, (8), pp. 2939–2942

[9] Zou, Z., Cui, X., Lu, T.: 'Measurement method of charge densities at ground level under high-voltage direct current conductor', *IET Sci. Meas. Technol.*, 2015, **9**, (8), pp. 973–978

[10] Xie, L., Zhao, L., Lu, J., *et al.*: 'Altitude correction of radio interference of HVDC transmission lines part I: converting method of measured data', *IEEE Trans. Electromagn. Compat.*, 2017, **59**, (1), pp. 275–283

[11] Zhao, L., Cui, X., Xie, L., *et al.*: 'Altitude correction of radio interference of HVdc transmission lines part II: measured data analysis and altitude correction', *IEEE Trans. Electromagn. Compat.*, 2017, **59**, (1), pp. 284–292

[12] Li, X., Cui, X., Lu, T., *et al.*: 'Experimental investigation on correlation of corona-induced vibration and audible noise from DC conductor', *High Voltage*, 2016, **1**, (3), pp. 115–121

[13] Zhao, L., Lu, J., Cui, X., *et al.*: 'The altitude effect and correction of audible noise for HVDC transmission lines', *IEEE Trans. Power Deliv.*, 2017, **32**, (4), pp. 1954–1963

[14] Yuan, H., Yang, Q., Liu, Y., *et al.*: 'Development and application of high-frequency sensor for corona current measurement under ultra high-voltage direct-current environment', *IEEE Trans. Instrum. Meas.*, 2012, **61**, (4), pp. 1064–1071

[15] Bian, X.M., Wan, S.W., Liu, L., *et al.*: 'The role of charged particles in the positive corona-generated photon count in a rod to plane air gap', *Appl. Phys. Lett.*, 2013, **103**, (9), p. 094102

[16] Bian, X., Wang, L., Liu, Y., *et al.*: 'High altitude effect on corona inception voltages of DC power transmission conductors based on the mobile corona cage', *IEEE Trans. Power Deliv.*, 2013, **28**, (3), pp. 1971–1973

[17] Bian, X.M., Chen, L., Yu, D.M., *et al.*: 'Surface roughness effects on the corona discharge intensity of long-term operating conductors', *Appl. Phys. Lett.*, 2012, **101**, (17), p. 174103

[18] Cui, Y., Wang, Q., Yuan, H., , *et al.*: 'Relative localization in wireless sensor networks for measurement of electric fields under HVDC transmission lines', *Sensors*, 2015, **15**, (2), pp. 3540–3564

[19] Cheung, K.W., So, H.C., Ma, W.-K.: 'Least squares algorithms for time-of-arrival-based mobile location', *IEEE Trans. SIGNAL Process.*, 2004, **52**, (4), pp. 1121–1128

[20] Sun, M., Yang, L., Ho, D.K.C.: 'Efficient joint source and sensor localization in closed-form', *IEEE Signal Process. Lett.*, 2012, **19**, (7), pp. 399–402

[21] Liu, H., Darabi, H., Banerjee, P., *et al.*: 'Survey of wireless indoor positioning techniques and systems', *IEEE Trans. Syst. Man Cybern. Part C Appl. Rev.*, 2007, **37**, (6), pp. 1067–1080

[22] Paul, S., Wan, E.: 'RSSI-based indoor localization and tracking using sigma-point kalman smoothers', *IEEE J. Sel. Top. Signal Process.*, 2009, **3**, (5), pp. 860–873

[23] Liu, L.C., Wu, K.W.K., He, T.H.T.: 'Sensor localization with ring overlapping based on comparison of received signal strength indicator'. 2004 IEEE Int. Conf. Mob. Ad-hoc Sens. Syst., pp. 516–518

[24] Wang, S., Inkol, R., Jackson, B.R.: 'Relationship between the maximum likelihood emitter location estimators based on received signal strength (RSS) and received signal strength difference (RSSD)'. 2012 26th Bienn. Symp. Commun. QBSC 2012, vol. **2**, (2), pp. 64–69

[25] Cui, Y., Lv, J., Yuan, H., *et al.*: 'Development of a wireless sensor network for distributed measurement of total electric field under HVDC transmission lines', *Int. J. Distrib. Sen. Netw.*, 2014, **10**, (5), p. 850842

[26] Cui, Y., Yuan, H., Song, X., , *et al.*: 'Model, design and testing of field mill sensors for measuring electric fields under high-voltage direct current power lines', *IEEE Trans. Ind. Electron.*, 2017, DOI: 10.1109/TIE.2017.2719618

[27] Li, X.: 'RSS-based location estimation with unknown pathloss model', *IEEE Trans. Wirel. Commun.*, 2006, **5**, (12), pp. 3626–3633

[28] Gungor, V.C., Lu, B., Hancke, G.P.: 'Opportunities and challenges of wireless sensor networks in smart grid', *IEEE Trans. Ind. Electron.*, 2010, **57**, (10), pp. 3557–3564

[29] Gezici, S.: 'A survey on wireless position estimation', *Wirel. Pers. Commun.*, 2008, **44**, pp. 263–282